Assessment of the impact of frequency support on DFIG wind turbine loads

Barahona Garzón, Braulio; You, Rui; Hansen, Anca Daniela; Cutululis, Nicolaos Antonio; Sørensen, Poul Ejnar

Published in:
12th International Workshop on Large-Scale Integration of Wind Power into Power Systems as well as on Transmission Networks for Offshore Wind Power Plants

Publication date:
2013

Assessment of the impact of frequency support on DFIG wind turbine loads

Braulio Barahona[1*], Rui You[2], Anca D. Hansen[1], Nicolaos A. Cutululis[1], and Poul Sørensen[1]
[1]DTU Wind Energy
Technical University of Denmark
4000 Roskilde, Denmark
[*]Email: brab@dtu.dk
[2]State Key Laboratory of Control and Simulation of Power System and Generation Equipment
Department of Electrical Engineering, Tsinghua University
100084 Beijing, China

***Abstract*—This study presents models and tools for the assessment of the impact that providing frequency support has on doubly-fed generator (DFIG) wind turbine structural loads and drive train. The focus is on primary frequency support, aiming at quantifying the impact on wind turbines acting as frequency containment reserve and providing inertial response. The sensitivity of wind turbine load indicators—load-duration-distribution and maximum load values—to inertial response control actions and different torsional models of drive train is investigated. The analysis is done by co-simulations of an aeroelastic code and electrical models. In this simulation framework, the impact that power system conditions can have on wind turbines, and vice versa the support that wind turbines can offer to the power system can be investigated.**

I. Introduction

The context is now set for wind power plant ancillary services, such as frequency support, to take a relevant role in the operation of power systems. Therefore, for wind power plant developers it is important to estimate the capability of a wind power plant to provide a service and the cost that such a service would have. Part of this cost can be related to reduction of wind turbine life time or increased maintenance. In this study we present models and tools that can be used to estimate the impact that providing frequency support can have on doubly-fed generator (DFIG) wind turbine structural loads and drive train. An integrated simulation approach [1] is applied, which provides a simulation framework for the analysis of wind turbine response—aeroelastic, drive train and electrical dynamics—while estimating the capability of the wind power plant to support the power system frequency.

In the technical literature, it is widely proposed that given a sudden, and large unbalance of the power system active power, wind turbines can respond to help controlling the frequency within the system operator limits in order to avoid load shedding or system collapse. The inertial response of wind turbines to power system frequency changes may be intrinsic (i.e. fixed-speed), or controlled (i.e. variable-speed wind turbines). Regarding the time frame of the response, and purpose of the control the simplest categorization of frequency response may be

- instantaneous to within a few seconds (i.e. inertial response, primary response), or
- more than a few seconds after the event once the frequency is again stable, but not it is not yet at its nominal value (i.e. secondary response).

The focus in this work is on inertial response, with the aim at quantifying the impact on wind turbines acting as frequency containment reserve [2] (the ENTSO-E designation for primary reserve) and providing fast frequency response.

Next Section describes the models used for this work, Section III describes simulations and results and Section IV presents the conclusion from this work.

II. Model for integrated analysis

An aeroelastic model of a horizontal axis wind turbine is coupled to electrical models of controls, generator and power system as illustrated in Figure 1. A classical power system model for frequency control studies—which considers the lumped response of generation and load, and speed regulation—is connected to a wind power plant model. The wind power plant is represented by the upscaled response of a single wind turbine of megawatt size, which is aggregated assuming that the power outputs from the wind turbines are identical stochastic processes, normally distributed and uncorrelated.

The wind turbine model consists of aeroelastic model, torsional representation of drive train—low speed shaft, gearbox, high speed shaft—dynamic model of asynchronous generator, power electronics are considered ideal, and control system—blade pitch angle and generator. The analysis is done by co-simulations with the aeroelastic code HAWC2 and the software Matlab/Simulink. This co-simulation framework sets a non-iterative coupling—which is appropriate for coupling aeroelastic and electro-mechanical systems—between the solver in the aeroelastic code and the one in Matlab, it lets both software stand alone and takes advantage of variable step solvers in Matlab [1].

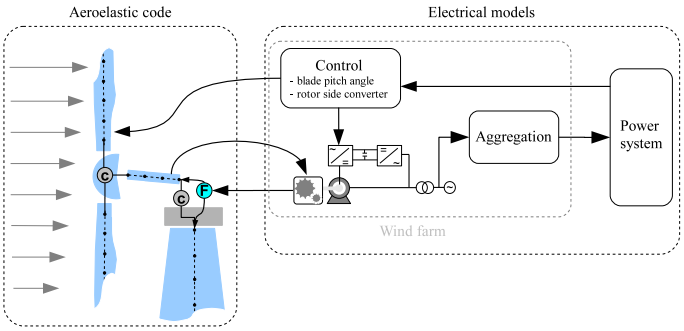

Figure 1. Model for integrated analysis: aeroelastic code HAWC2 is coupled to electrical models in Matlab/Simulink.

A. Power system model for frequency support

The power system model is based on the premise that active and reactive power flows are practically independent in transmission systems [3]. Under this consideration, active power balance influences the power system frequency—and not the voltage. The model, illustrated in Figure 2, considers the lumped response of generation and load, and speed regulation.

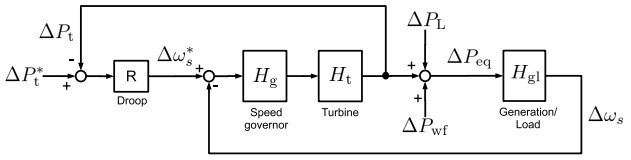

Figure 2. Power system model for frequency control in delta variables.

1) Generation and load: the response in frequency (i.e. $\Delta\omega_s$) of generation and loads in a power system, to changes in the power balance ΔP_{eq} can be represented as a first-order system [3]. The time constant of such equivalent system is a *lumped* inertia constant M_{gl}, that is the sum of the inertia constants of the generating units in the power system in question. The damping provided by the loads in the system is lumped in a damping constant D_{gl}. The transfer function of this representation of generation and load in a power system is given in Equation 1.

$$H_{\text{gl}}(s) = \frac{1}{M_{\text{gl}}s + D_{\text{gl}}} \tag{1}$$

2) Speed governing: the control of the generation units is modeled as a typical speed governor and turbine. The *speed governor* consists of a PI control of speed, the set point is calculated with the linear relation of changes in load to speed deviation—*droop* of speed-to-load, or speed regulation characteristic—the output is a command to the turbine to increase or reduce production accordingly. Equation 2 is the transfer function of the PI control of speed, where K_{pg} is the proportional gain and K_{ig} the integral gain.

$$H_{\text{g}}(s) = \frac{K_{\text{pg}}s + K_{\text{ig}}}{s} \tag{2}$$

The prime movers are represented as a first order system with a time constant τ_{t}, has shown in Equation 3.

$$H_{\text{t}}(s) = \frac{1}{\tau_{\text{t}}s + 1} \tag{3}$$

The implementation of the frequency control power system model is done in delta variables as shown in Figure 2, where $\Delta\omega_s$ is the deviation of the system frequency from the synchronous value. ΔP_{eq} represents the active power balance between generation and load, ΔP_{L} changes in load, and ΔP_{wf} the changes in power from wind power plants.

B. Aerodynamics and structure

A wind turbine aeroelastic model represents the dynamics of the wind turbine rotor and structure coupled to the aerodynamic forces created by the interaction with the wind field. The aeroelastic code HAWC2 is used in this work, which has a multibody dynamics formulation in a floating reference frame, allowing large rotations and deflections to be properly considered. The structural subsystems are composed of bodies, each of them composed of a number of Timoshenko three-dimensional beams with their own coordinate system (elements with 6 degrees-of-freedom). Bodies have a set of algebraic equations—constraints—which relate their movements, and forces to those of other bodies. Constraints are solved together with the equations of motion (second order, non-linear differential equations) [4]. The aerodynamic forces are calculated with blade element momentum method, including dynamic stall and tower shadow effects. The wind field has logarithmic shear and Mann turbulence.

A multibody structural model is illustrated in Figure 3, where one of the blades, and the tower are represented with their main bodies, constraints, and external forces (i.e. generator torque, or torque at the low speed shaft).

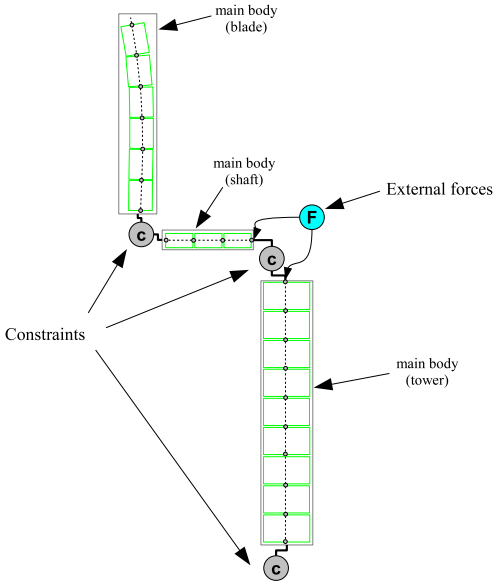

Figure 3. Structural model and low-speed shaft part of drive train in HAWC2

C. Gearbox torsional models

Gearboxes are very complex mechanical systems, whose modelling and analysis for design purposes is done mainly by finite element. At the system level, a torsional representation can be sufficient to represent the overall dynamics and perhaps—together with considerations about various deterministic and stochastic operating conditions—to give enough insight about the operating conditions to proceed with detail level design. Torsional models can also be used for controller design, for example in [5] a four degree of freedom model, similar to one we describe below, of a typical 3 stage wind turbine gearbox is used to design a load reduction control. These models represent the torsional degrees of freedom building from rigid body representation of mechanical systems by a series of lumped masses (rotational inertias) connected by springs and dampers.

1) 2 DOF: this model represents a gearbox as a two rotational inertias (J_1, J_2) connected by a torsional stiffness k and damping c, with a gear ratio η, speed at low-speed

ω_1 and at high-speed ω_2 gears and input torques T_1 and T_2.

$$\dot{\omega}_1 = \frac{-c}{J_1}\omega_1 + \frac{c}{\eta J_1}\omega_2 - \frac{k}{J_1}\vartheta + \frac{T_1}{J_1} \tag{4}$$

$$\dot{\omega}_2 = \frac{c}{\eta J_2}\omega_1 - \frac{c}{\eta^2 J_2}\omega_2 + \frac{k}{\eta J_2}\vartheta - \frac{T_2}{J_1} \tag{5}$$

$$\dot{\vartheta} = \omega_1 - \frac{\omega_2}{\eta} \tag{6}$$

2) 4 DOF: a typical 3 stage gearbox is illustrated in Figure 4, representing the gears of each stage (*A*, *B*, and *C*) as lumped rotational inertias connected by shafts (s_1, s_2, and s_3) with their corresponding torsional stiffness and damping.

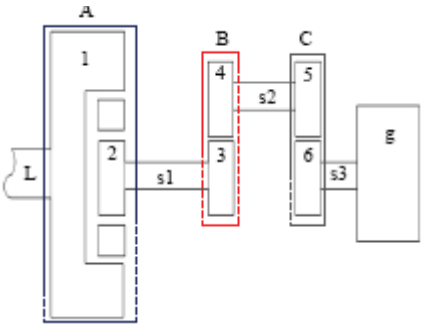

Figure 4. 4 DOF torsional model of typical 3 stage gearbox.

Equations 7 describe the dynamics of the 4 degrees of freedom, corresponding the speed of the lumped mass of each stage (ω_A, ω_B and ω_C) and the twist angle of each shaft (ϑ_{AB}, ϑ_{BC} and ϑ_{Cg}), subject to the input torques at low-speed side T_L and from the generator T_g. All of them are referred to the low speed shaft by the corresponding gear ratios η.

$$\begin{aligned}
\dot{\omega}_A &= \frac{-c_{s1}}{J_A}\omega_A + \frac{c_{s1}}{\eta_1 J_A}\omega_B - \frac{k_{s1}}{J_A}\vartheta'_{AB} + \frac{T_L}{J_A} \\
\dot{\omega}_B &= \frac{\eta_1 c_{s1}}{J_B}\omega_A - \frac{c_{s1}+c_{s2}}{J_B}\omega_B + \frac{c_{s2}}{\eta_2 J_B}\omega_C + \ldots \\
&\quad \ldots + \frac{\eta_1 k_{s1}}{J_B}\vartheta'_{AB} - \frac{\eta_1 k_{s2}}{J_B}\vartheta'_{BC} \\
\dot{\omega}_C &= \frac{\eta_2 c_{s2}}{J_C} - \frac{c_{s2}+c_{s3}}{J_C}\omega_C + \frac{c_{s3}}{\eta_3} \\
\dot{\omega}_g &= \frac{c_{s3}}{(\eta_1\eta_2)^2 J_g}\omega_C - \frac{c_{s3}}{(\eta_1\eta_2\eta_3)^2 J_g}\omega_g + \ldots \\
&\quad \ldots + \frac{k_{s3}}{\eta_1\eta_2\eta_3 J_g}\vartheta'_{Cg} - \frac{T_g}{J_g} \\
\dot{\vartheta}'_{AB} &= \omega_A - \frac{\omega_B}{\eta_1} \\
\dot{\vartheta}'_{BC} &= \frac{\omega_B}{\eta_1} - \frac{\omega_C}{\eta_1\eta_2} \\
\dot{\vartheta}'_{Cg} &= \frac{\omega_c}{\eta_1\eta_2} - \frac{\omega_g}{\eta_1\eta_2\eta_3}
\end{aligned} \tag{7}$$

D. Doubly fed electrical generator

A classical reduced order model of an asynchronous machine in *dq*-frame is used, which is formulated with the voltage equations in terms of flux linkages [6]. The reduced order model consists in neglecting the stator fluxes transients. Therefore it includes only the states corresponding to the rotor fluxes, and the stator fluxes are solved with algebraic equations, as shown here in matrix form with Equation 8

$$\begin{bmatrix} \mathbf{0} \\ \dot{\lambda}_{dqr} \end{bmatrix} = \mathscr{M} \begin{bmatrix} \lambda_{dqs} \\ \lambda_{dqr} \end{bmatrix} + \begin{bmatrix} \mathbf{v}_{dqs} \\ \mathbf{v}_{dqr} \end{bmatrix} \tag{8}$$

where

$$\mathscr{M} = -\left(\mathbf{R}\mathbf{L}_{dq}^{-1} + \Omega\right) \tag{9}$$

$\mathscr{M}$ is a matrix derived from the equivalent circuit of the machine and the transformation and reference frame chosen.

The rotor circuit is connected to the grid by a back-to-back converter. The direct current link and the grid side converter are considered ideal in this work, while the rotor side converter and its control are modelled by a cascade of proportional integral control loops in *dq*-frame, one of them controlling active power (or torque) and the other controlling reactive power. Figure 5 shows the active power control loop.

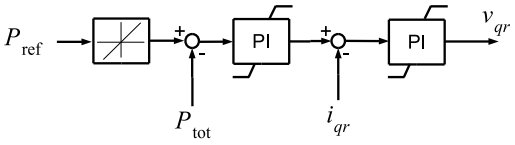

Figure 5. Rotor side converter control: q-loop.

E. Blade angle control

The pitch blade angles are controlled by a deterministic adaptive control, implemented according to [7]. A block diagram of such control is shown in Figure 6. It consists of a PI regulator with a scheduled gain. The schedule of the gain is designed to compensate nonlinear aerodynamic characteristics. The servo motors that rotate the blades are represented as a first order system with limits to minimum-maximum blade angle, and blade angle rate of change.

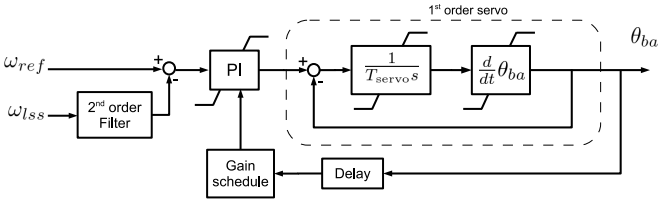

Figure 6. Blade angle control for variable-speed wind turbine.

F. Inertial response control

Inertial response can be provided by wind turbines to support a power system on conditions of sudden loss of generation. However, in the case of variable-speed wind turbines (VSWTs), auxiliary control loops are needed in order to provide an adequate inertial response. Demonstration of control concepts that tap kinetic energy of a wind turbine rotor to *emulate* an inertial response, has been done in several publications. All of them based on the fundamental relationship between rotational speed, and kinetic energy. For example, the work in [8] derived an *inertial response* control

law to tap kinetic energy from the wind turbine rotor, as indicated in Equation 10

$$T_{\text{ir}}^{*} = 2H_{\text{wt}}\dot{\omega}_s \tag{10}$$

where H_{wt} is the so-called *inertia constant* [3], and $\dot{\omega}_s$ is the time derivative of frequency of power system voltage. Observe that in Equation 10 a negative slope of $\omega_s(t)$ yields a negative torque T_{ir}^{*}. The inertia constant of wind turbines is, in this study defined by Equation 11, where J_{wt} is the lumped moment of inertia of the wind turbine rotor J_{rot} plus the moment of inertia of the generator rotor J_{gen}. In drive trains with gearbox, J_{rot} is referred to the high-speed side (i.e. to the mechanical speed of the generator rotor). ω_{sm} is the *mechanical* synchronous frequency, and S_{base} is the apparent power base of the generator.

$$H_{\text{wt}} = \frac{J_{\text{wt}}\omega_{sm}^{2}}{2S_{\text{base}}} \tag{11}$$

The implementation of the control law for inertial response (Equation 10) in [8], [9], includes a first order filter of $\dot{\omega}_s$ that is said to limit rate of change, and the maximum peak of torque. Such implementation is illustrated in Figure 7, where the torque set point T_{ir}^{*}, calculated with the inertial response control law, is subtracted to a torque set point T_{ref}, calculated from the torque-speed operation curve of the wind turbine. T_{ref} is then converted to a current set point i_{qr}^{*}, that is the input to the current control loop. In [10], the same approach is taken but instead of a filter, a compensation element $k/(s^2+2\xi\omega_n s+\omega_n^2)$ is used.

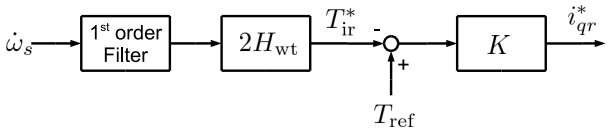

Figure 7. Inertia response control—based on torque set point.

In [9] the inertial response control in Figure 7 is compared to a control proportional to the deviation of the frequency to its nominal value—*droop control*—given by Equation 12.

$$T_{dr}^{*} = k_{dr}(\omega_0 - \omega_s) \tag{12}$$

Similarly, [11], [12] utilize a power set point P_{ir} to tap the kinetic energy of the wind turbine rotor. This control law is illustrated in Figure 8. The limits to the inertial response power set point P_{ir} are $P_{\text{ir}}^{\min}$, $P_{\text{ir}}^{\max}$. The limits to the rate of change of P_{ir} are $(\frac{d}{dt}P_{\text{ir}})^{\min}$, and $(\frac{d}{dt}P_{\text{ir}})^{\max}$. P_{ref}^{*} is the optimal power set point, and P_{ref} the set point to the generator power control loop.

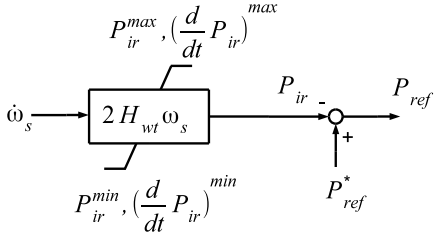

Figure 8. Inertia response control based on power set point.

III. Simulation results

The co-simulation environment and models presented are used for integrated analysis of a 2 MW DFIG turbine, within a wind power plant connected to a large power system. This approach facilitates the analysis of the impact of wind turbines on the power system and vice versa.

A. Power system frequency

When a generator outage happens in the power system, the frequency of the power systems drops while the speed governors of the conventional power plants react by increasing their power production; as shown in Figure 9 by the black line. It is expected that wind power plants will be able to support in a similar manner, improving the support to the power system frequency. This is also shown in Figure 9 for cases when the wind power plant with inertial response control is operating at low wind speed and when the wind speed is high, above rated. The influence of increasing the gain H_{wt} in the inertial response control, which represents the wind turbine inertia, is also illustrated.

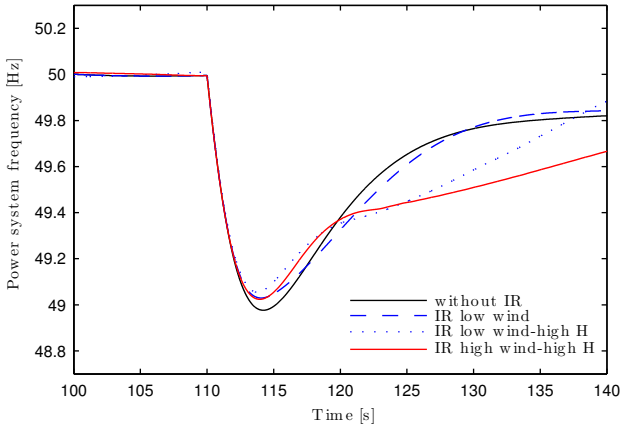

Figure 9. Power system frequency during generation loss of 8%, without and with inertial response from wind turbines. Low wind speed case is 7.5 m/s and high wind speed is 15 m/s with 10 % turbulence intensity.

B. Wind turbine loads

With the integrated models presented, the wind turbine structural and drive-train loads can be analyzed with different levels of detail under realistic external conditions. In the context of this work, investigations of wind turbine loads was done in different points of the power curve for cases of de-loaded operation to provide primary frequency support, and maximum production with inertial response control. In the following we present the case of inertial response while the turbine is operating at lower wind speeds in normal conditions (i.e., maximum production). In this case, the torque set point to the wind turbine is based on maximum power tracking point and the inertial response control.

Figure 10 shows time series of electromagnetic torque, drive-train and structural loads for different gearbox models. Observe how as the wind turbine is required to provide more power, the electromagnetic torque increases—therefore the wind power plant total output also increases to support the

power system—which influences torque and speed throughout the drive train, and to some extend the tower side-to-side moment. This is shown in the middle and bottom plots of Figure 10. Notice also that the 4 DOF gearbox model introduces more fluctuations on the shaft torsion and tower side moment than other models, while the maximum values are very close.

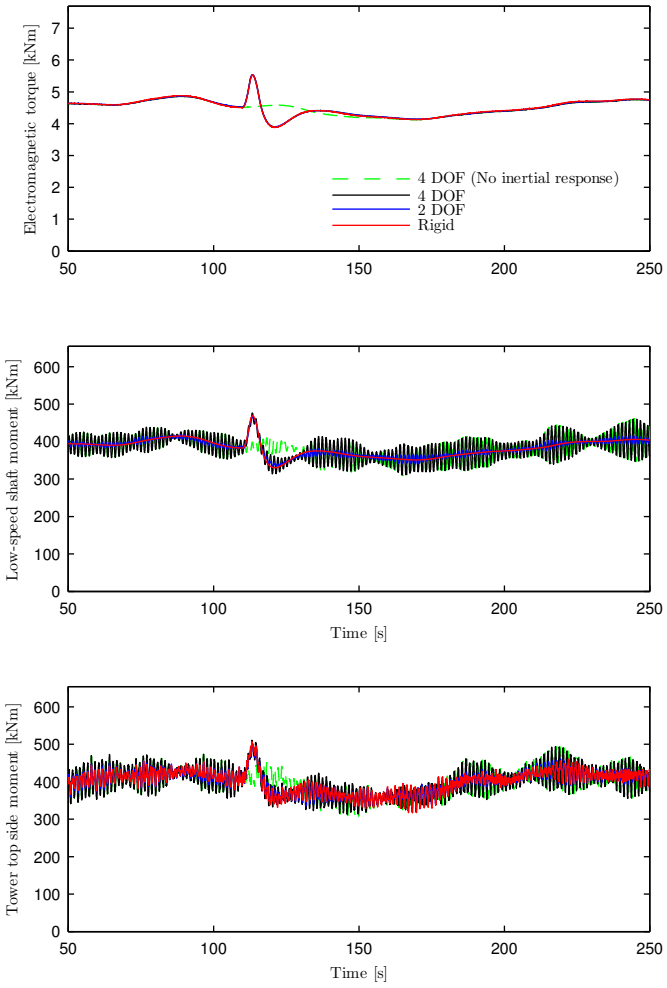

Figure 10. Wind turbine electromagnetic torque (top), low-speed shaft (middle) and tower top side-to-side moment (bottom) during generation loss of 8% with different models of gearbox, mean wind speed at hub height is 7.5 m/s with 10 % turbulence intensity.

Figure 11, shows the load duration distribution (LDD) [13] of the previous time series of torque at the low speed shaft (top plot) and side-to-side moment of the tower top (bottom plot). It can be observed, that the inertial response control increases the maximum values about 13-15 % and 10 % respectively. Although the maximum values are practically the same for the different gearbox models in this case, the 4 DOF model shows slightly higher levels of load for duration up to 50 seconds, which in the long term could be important for fatigue. Therefore, it is necessary to validate the accuracy of torsional models and how well they represent the dyanmics of drive train and how load is transferred to the tower.

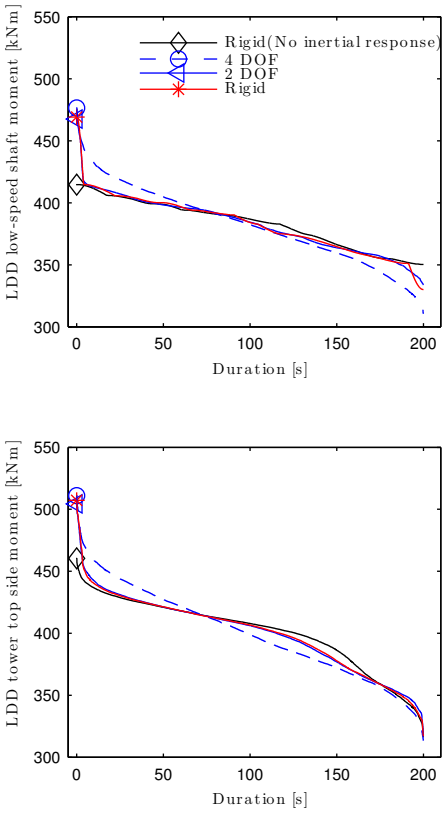

Figure 11. Load distribution of low-speed shaft torsion (top) and tower top side-to-side moment (bottom) during generation loss of about 8% with different models of gearbox, mean wind speed at hub height is 7.5 m/s with 10 % turbulence intensity.

IV. Discussion and Conclusions

A co-simulation environment that couples an aeroelastic code (HAWC2) to electrical models in Matlab/Simulink was applied to study the dynamics of DFIG wind turbines during inertial response, while at the same time being able to observe the impact on the power system frequency. Since wind power plants are nowadays operating under complex environmental conditions and demanding electrical requirements, reliable and cost effective wind turbine designs—which are compliant with grid codes—are necessary. Therefore in this work, we analyzed the impact that providing inertial response to support power system frequency can have on wind turbine loads. A case of inertial response at low wind speed was presented. Simulations show that the maximum values of shaft torsion and tower top side-to-side moment can be affected, increasing in about 10 % compared to maximum values in normal operation, when the wind power plant is not supporting the power system. Different gearbox torsional models were used, showing minor differences in the maximum values and load duration distribution for the case presented. In this direction, it follows to investigate the value of this type of analysis (with models of different degree of simplicity) for the design of drive train components. For example, by defining relevant input from dynamic simulations to finite element analysis (or detailed multibody models) in order to benchmark different design cases with those derived from power conditions. Another important aspect is validation with measurements on megawatt size

wind turbines.

ACKNOWLEDGMENT

This work is partly supported by the REserviceS project funded by Intelligent Energy - Europe (IEE programme). The financial support provided by China Scholarship Council (CSC) during a visit of Rui You to DTU Wind Energy is also acknowledged.

REFERENCES

[1] B. Barahona, "Integrated analysis of wind turbines —the impact of power systems on wind turbine design," Ph.D. dissertation, Technical University of Denmark, 2012.

[2] H. Holttinen, J. Kiviluoma, N. Cutululis, A. Gubine, A. Keane, and F. V. Hulle, "Ancillary services: technical specifications, system needs and costs," REserviceS - Economic grid support from variable renewables, European Wind Energy Association, Tech. Rep., 2012.

[3] P. Kundur, *Power System Stability and Control*. McGraw-Hill, 1994.

[4] B. S. Kallesøe, T. J. Larsen, and U. S. Paulsen, "Aero-Hydro-Elastic Simulation Platform for Wave Energy Systems and floating Wind Turbines," Risø DTU, Tech. Rep., 2011.

[5] A. Nasiri, E. Muljadi, G. Mandic, and F. Oyague, "Active torque control for gearbox load reduction in a variable speed wind turbine," 2012.

[6] C.-M. Ong, *Dynamic Simulation of Electric Machinery using Matlab/Simulink*. Prentince Hall PRT, 1998.

[7] A. D. Hansen and G. Michalke, "Fault ride-through capability of DFIG wind turbines," *Renewable Energy*, vol. 32, pp. 1594 – 1610, December 2006.

[8] J. Ekanayake and N. Jenkins, "Comparison of the response of doubly fed and fixed-speed induction generator wind turbines to changes in network frequency," *IEEE Transactions on Energy Conversion*, vol. 19, pp. 800 – 802, 2004.

[9] J. Morren, J. Pierik, and S. W. de Haan, "Inertial response of variable speed wind turbines," *Electric Power Systems Research*, vol. 76, pp. 980 – 987, 2006.

[10] L. Holdsworth, I. Charalambous, N. Jenkins, J. Ekanayake, J. Ekanayake, and N. Jenkins, "Power system fault ride through capabilities of induction generator based wind turbines," *Wind Eng.*, vol. 28, no. 4, pp. 399–409, 2004.

[11] N. R. Ullah, T. Thiringer, and D. Karlsson, "Temporary primary frequency control support by variable speed wind turbines - potential and applications," *IEEE Transactions on Power Systems*, vol. 23, pp. 601 – 612, 2008.

[12] G. C. Tarnowski, P. C. Kjær, P. E. Sørensen, and J. Østergaard, "Study on variable speed wind turbines capability for frequency response," in *European Wind Energy Conference*, 2009.

[13] B. Niederstucke, A. Anders, P. Dalhoff, and R. Grzybowski, "Load data analysis for wind turbine gearboxes," Germanischer Lloyd WindEnergie GmbH, Tech. Rep., 2003.